Statistical Analysis Approaches in Scour Depth of Bridge Piers

Shahad Abdulkathum [1], Hassan I. Al-Shaikhli [2]*, Ahmed A. Al-Abody [2],
Tameem M. Hashim [3]

[1] *General Directorate of Education Baghdad Rusafa Second, Ministry of Education, Baghdad, Iraq.*

[2] *Civil Engineering Department, College of Engineering, Warith Al-Anbiyaa University, Karbala, Iraq.*

[3] *Department of Building and Construction Techniques Engineering, Al-Mustaqbal University College, Babylon, Iraq.*

Abstract

A local scour is the removal of bed material from around the pier of the bridge. This bed removal is considered a big problem and is of great concern for hydraulic engineers. They should find economic solutions for this problem. The exaggerated local scour around bridge piers leads to many problems for the whole bridge structure, such as stability problems that may lead to the bridge's destruction. This paper aims to verify the scour depth around different shapes of uniform bridge piers for different flow conditions than those done by previous researchers using different prediction models. Where the consistency of previous experimental investigations is verified by multiple nonlinear regression analysis (MNLR), Gene Expression Programming (GEP) and Artificial Neural Network (ANN) models. In the comparison of values that were measured and predicted by the four models (CFD, MNLR, ANN, and Gene), it is seen that the ANN model has the ability to predict the Y_s/b values higher than other models used in relation to the measured values. This makes the ANN model superior in predicting the Y_s/b value over the other used models, followed by the Gene model. In comparison, the values of the R^2 and RMSE for the four models that were used in this study, for the Y_s/b model using the ANN had a value of 0.9978 and 0.0147, respectively, while those for the Y_s/b model using the Gene model were 0.9800 and 0.0375, respectively.

Keywords: Scour Depth Estimation; Local Scour; Empirical Formula; ANN; MNLR; GEP; CFD.

1. Introduction

"Scouring" means the sediment removal near or around the structures that are located in the flowing water (hydraulic structures). The sediment removal will cause a lowering in the river bed around the structure's foundation as a result of the water erosion. The high discharge passage may result in scouring. The foundation design must be strong enough to withstand the scouring effect because the failure of this part of the structure will destroy the whole structure. The depth of scour is an important factor in deciding the level of a bridge's foundation. Scouring results from the flowing water's erosive action, where it is excavated and carries the material from the bed around the bridge abutment and piers [1]. Many bridges have been damaged or collapsed as a result of the scouring problem, as documented in the literature. In New Zealand, one bridge on average every year fails because of scouring [2]. A study in 1973 for the Federal Highway Administration (FHWA), quoted by Arneson et al. (2012) [3], found that the flood caused 383 bridge collapses, about 25% because of pier damage and 75% because of abutment damage. Also in 1987, floods in New York and New England led to the destruction of 17 bridges [4].

Many factors have effects on bridge pier scouring and flow patterns. This paper focuses on the pier shape influence on local scour and how to minimize it. The pier shape is an important factor that plays a role in the creation and strength of the vortex system that is generated because the flowing water faces the pier or impacts with it. The vortex system can be divided according to the literature into wake vortex, horseshoe vortex, trailing vortex, and bow wave vortex [5]. Two kinds of piers are found in the literature: uniform piers (simple) and non-uniform piers (complex). The uniform piers are of a constant section along their depth, and non-uniform piers include slab footings, tapered piers, and piers of piled foundations [2]. This paper uses only uniform shapes and their influences on local scour depth.

Research studies have been published on local scour around bridge piers in the past few decades, especially by field observation or by physical modeling [6]. There are many difficulties in experimental studies related to scour patterns and flow fields that have developed around the hydraulic structures because of the technical limitations of the measuring devices. Also, because of the expensive price of these devices, such as an ultrasound velocity meter, the pier shape effect on local scour was studied by some researchers (e.g., Laursen & Toch (1956) [7], Neil et al. (2002) [8], Dietz (1972) [9], Melville (1975) [10], Komura et al. (1977) [11]). Many researchers have studied the circular pier shape extensively in the literature, including Melville (1975) [10], Chiew (1984) [5], Omara (2022) [12], Luo et al. (2022) [13], Reddy (2022) [14], Farooq & Ghumman (2019) [15], Jan & Lone (2022) [16], etc. The square-nose pier has the highest scour depth, and the sharp one has the lowest. Until recently, numerical modeling was extensively used in simulating the scour and flow patterns around the circular piers. Where the main use of numerical simulation is not needed to build a big model, there is no need to use an instrument like a velocimeter. The turbulence kinetic energy, bed shear stresses, and fluid behavior like velocity distribution can be determined by computational fluid dynamics (CFD) software such as Flow3D, Fluent, COMSOL, etc. The CFD programs were developed to solve scouring and fluid pattern behavior by solving the partial differential equations according to mass conservation, energy conservation, etc. Al-Shukur & Obeid (2016) [17] studied the effect of bridge pier shape on the depth and configuration of local scour. In their experimental study regarding bridge pier shape to minimize local scour, they used ten different pier shapes, as shown in Figure 1, and the schematic illustration of their experimental setup is shown in Figure 2. The experimental fume was 12 m long, 0.5 m wide, and 0.45 m high. They concluded that the rectangular pier is at maximum scour depth (7.6 cm) and the streamline pier is at a minimum scour depth of 3 cm. The second paper was on 3D numerical simulation of local scouring and velocity distributions around bridge piers of different shapes. In this paper, they used CFD code to simulate the flow and scour around the ten piers in paper one. They concluded that about (5.1%−9.8%) the range of error for predicting the scour depth is considered a good result and the CFD code is an effective tool in predicting scour depth around bridge piers.
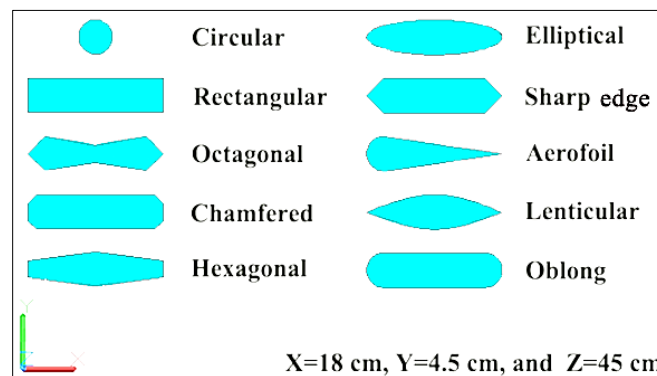

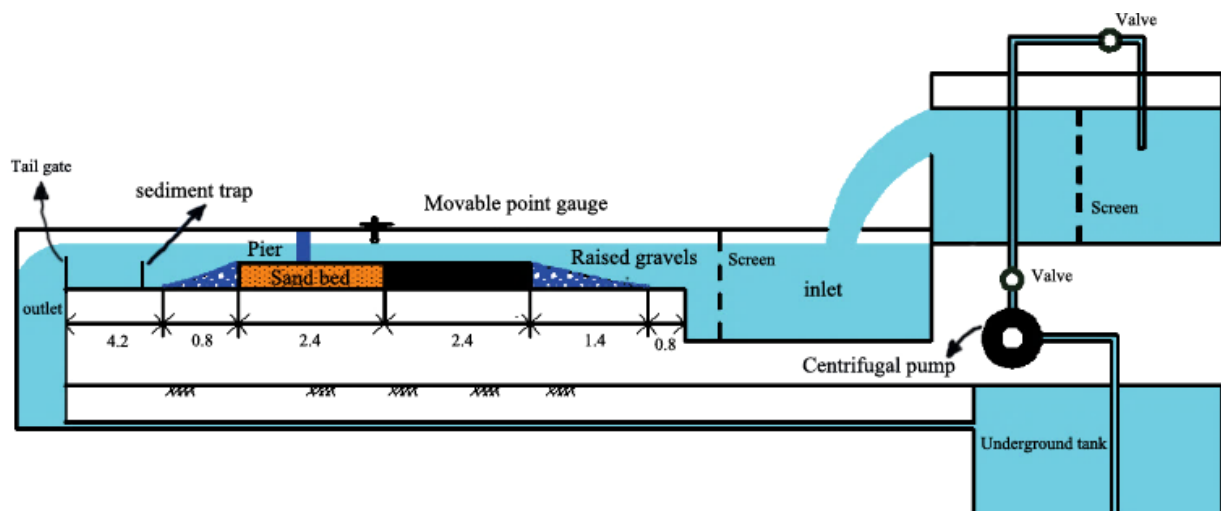**Figure 1. Piers models and dimensions**

Figure 2. The schematic illustration of experimental setup

This paper aims to verify the scour depth around different shapes of uniform bridge piers for different flow conditions, as done by Al-Shuker & Obeid (2016) [17] using different prediction models. Where the consistency of the experimental investigation is verified by multiple nonlinear regression analysis (MNLR), Gene Expression Programming (GEP) and Artificial Neural Network (ANN) models. To formulate prediction equations of equilibrium depth of local scour for ten pier shapes and examine the developed models in the experimental field.

According to a survey of the relevant published research, several distinct configurations of bridge piers and pile caps have been investigated in great detail with the intention of reducing scour in the immediate area. The effects of different pile shapes within a group, on the other hand, have not been studied in great detail. Researchers conducted experimental research on the scour that occurs around a complex pier that has a lenticular or elliptical pile cap. It has been demonstrated that the elliptical pile cap can successfully cut down on scour. On the other hand, observations made in the field have shown that the vast majority of the time, the earth is piled up to the top, and the shape of the pile cap is irrelevant to the process [18–23].

2. Dimensional Analysis

Dimensional analysis is an efficient technique used to translate the phenomenon behavior into a mathematical model or empirical equation. The physical regime of local scour around bridge piers cannot be understood accurately unless the correct dimensionless parameters describing the phenomenon are chosen in the proper way. The variables, which affect the local scour can be summarized in Equation 1 and illustrated in Table 1.

$$f\left(y_s. \rho. \mu. V. y. g. \rho_s. d_{50}. \sigma_g. V_c. S_o. G. b. L. K_s. \theta. t\right) = 0 \tag{1}$$

Table 1. The classification of parameters that affect the local scour mechanism in (MLT) system

	1) **Parameters characterizing the flow**	**Units**	**Dimensions**
P	Density of the fluid	kg/m³	ML^{-3}
N	Kinematic viscosity of the fluid	m²/s	L^2T^{-1}
G	Gravitational acceleration	m/s²	LT^{-2}
Y	Approach flow depth	m	L
V	Approach flow velocity	m/s	LT^{-1}
V_c	Critical mean approach flow (threshold velocity for sediment movement)	m/s	LT^{-1}
	2) **Parameters characterizing the bed material**	**Units**	**Dimensions**
ρ_s	Density of the sediment	kg/m³	ML^{-3}
d_{50}	Median sediment size	mm	L
σ_g	Standard deviation of particle size distribution	-	-
	3) **Parameters characterizing the flume**	**Units**	**Dimensions**
S_o	Channel bed slope	-	-
G	Channel width	m	L
	4) **Parameters characterizing the pier**	**Units**	**Dimensions**
L	Pier length	m	L
B	Pier diameter or pier width	m	L
K_s	Pier shape factor	-	-
β	Angle of approach flow to the axis	-	-
	5) **Time**	**Units**	**Dimensions**
T	Duration of flow	min	T

According to the π- theorem, there are three repeated variables are selected and fourteen dimensionless groups are obtained, the repeated parameters where ρ, V, and B, the general formula can be written in form of Buckingham π-theorem as shown in Equation 2.

$$f_1\left(\pi_1. \pi_2. \pi_3. \pi_4. \pi_5. \pi_6. \pi_7. \pi_8. \pi_9. \pi_{10}. \pi_{11}. \pi_{12}. \pi_{13}. \pi_{14}\right) \tag{2}$$

After the analyses have completed, the dimensionless groups that result from Buckingham π-theorem where $\pi_1 = \frac{y_s}{b}$, $\pi_2 = K_s$, $\pi_3 = \beta$, $\pi_4 = \frac{L}{b}$, $\pi_5 = \frac{y}{b}$, $\pi_6 = \frac{d_{50}}{b}$, $\pi_7 = \frac{G}{b}$, $\pi_8 = \frac{\rho_s}{\rho}$, $\pi_9 = \frac{V_c}{V}$, $\pi_{10} = \frac{V^2}{gb}$, $\pi_{11} = \frac{Vb}{v}$, $\pi_{12} = \sigma_g$, $\pi_{13} = S_o$, $\pi_{13} = \frac{\rho_s}{\rho}$, $\pi_{14} = \frac{Vt}{b}$.

For the situations of this study, the only one-bed material is used and equilibrium scour depth is being considered, the terms σ_g and Vt/b can be ignored. The angle of attack is zero in all experiments (β=0°). The term y/b is constant for

all experiments so it is dropped. The pier diameter b=45 mm and the median particle size d_{50}=0.71 mm. As b/d_{50}> 25 [24], the effect of this term is neglected. Also, the term V_b/v, usually is the insignificant parameter and can be neglected if the flow is fully turbulent around the pier [12]. Densities of the fluid and sediment are constant throughout the study. In this way, relative density term ρ_s/ρ is dismissed. The width of the flume is more than 6.25 times of the pier width to avoid the wall friction factor, proposed by Raudkivi & Ettema (1983) [25], so the term G/b is dropped. Since the flume slope is fixed at horizontal (i.e., S_o =0). Thus the S_o has no effect on the scour process. All models have the same length and projected width for flow, so the ratio L/b has no effect on equilibrium scour depth, so that, the general formula can be simplified and stated as shown in Equation 3:

$$\frac{y_s}{b} = f_1\left(\frac{V_c}{V} . K_s . \frac{V}{\sqrt{gb}}\right) \tag{3}$$

where, the term $\frac{V}{\sqrt{gb}}$ is known as pier Froude number (Fr_p).

3. Multiple Nonlinear Regression Approach (MNLR)

The multiple non-linear regression statistical approach was used to generate prediction models to estimate the scour depth depending on the experimental data [26]. The confidence of suggested relationships is evaluated according to the regression coefficient (R^2). The IBM SPSS Statistics 22 software was used to calculate the parameters of the suggested relationships. The regression coefficient can be calculated as [27]:

$$R^2 = 1 - \frac{\sum_{i=1}^{n}(y_o - y_p)^2}{\sum_{i=1}^{n}(y_o - \bar{y})^2} \tag{4}$$

where, R^2 is the regression coefficient, y_o is the observed value, y_p is the predicted value, $\bar{y}$ is the mean value of y_o and n is the number of data. The following equation form is suggested to predict the depth of scour including the effect of shapes depending on the experimental investigation:

$$y_{s/b} = a \times \left(\frac{v_c}{v}\right)^b \times (K_{sh})^c \times (Fr_p)^d \tag{5}$$

After analysing the experimental data using SPSS program, it got on the following equation:

$$y_{s/b} = 0.465 \times \left(\frac{v_c}{v}\right)^{2.9} \times (K_{sh})^{0.7} \times (Fr_p)^{-1.7} \tag{6}$$

where the R^2 of this equation is 0.961. The predicted versus observed values of scour depth are shown in Figure 3.
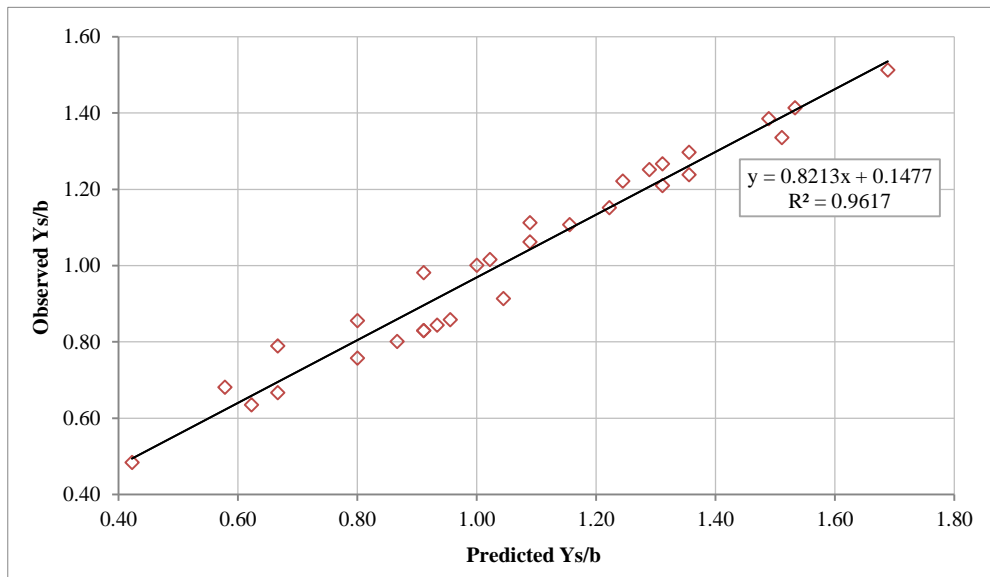

Figure 3. Predicted- Observed fitted line of MNLR Results

4. Artificial Neural Network Approach (ANN)

The artificial neural network (ANN) is a computing system that is considered a nonlinear statistical data modeling tool. This system is designed to solve the most complex problems and simulate the way the human brain processes and analyzes information. ANN is used to predict the scour depth in this study by interpolating and extrapolating the data [28]. It consists of three independent layers, namely input, hidden, and output layers. In the input layer where the input data inserted to the ANN and in the hidden layer the data is processed and specifies the type if single or multiple

layers. Then the output layer finally presents the ANN result that was produced. Each of these layers comprises many processing neurons. Every neuron in a layer works in a logical similarity. Information is transferred from one layer to another in serial operations. The most widely used in literature, the training algorithm for neural networks are forward and backward quick propagation algorithm. In this paper, we used the forward type. Also, in every neuron, there is a specific mathematical function known as the activation function. This function accepts the input from prior layers and generates the output for the second one. The layers are interconnected by weights. In this paper, the sigmoid activation function was used to represent the data obtained from the experimental work by Al-Shuker & Obeid (2016) [17]. Weights were calculated using the Quick Propagation Algorithm (QP), and the connection between neurons of each layer was Multiplayer Normal Feed Forward (MNFF) to solve and transfer the experimental data.

4.1. ANN Results

In this study, the activation function is a sigmoid function that was used to represent the experimental data of local scour depth. The Quick Propagation Algorithm (QP) used to calculate the weights of the artificial neural network (ANN) and the connection lines between ANN neurons is Multiplayer Normal Feed Forward (MNFF) for transferring and solving the data in each layer of the ANN structure, as shown in Figures 4 and 5, which illustrate the neural connection weights of the artificial neural network (ANN). Figure 6 illustrates the predicted-observed fitted line of the ANN model R^2 = 0.9978.
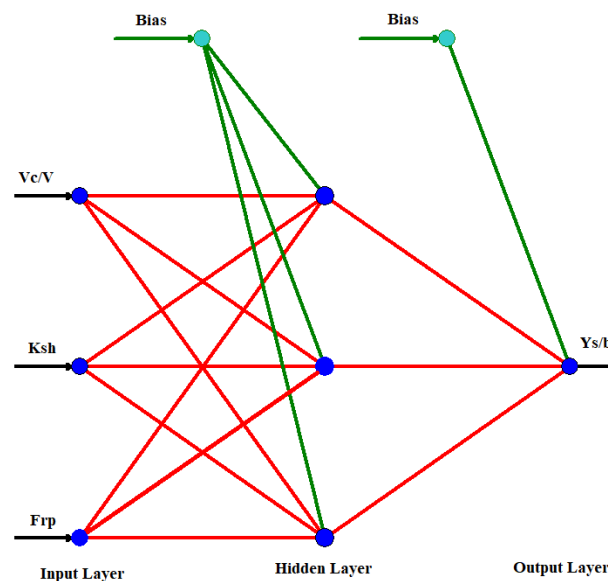

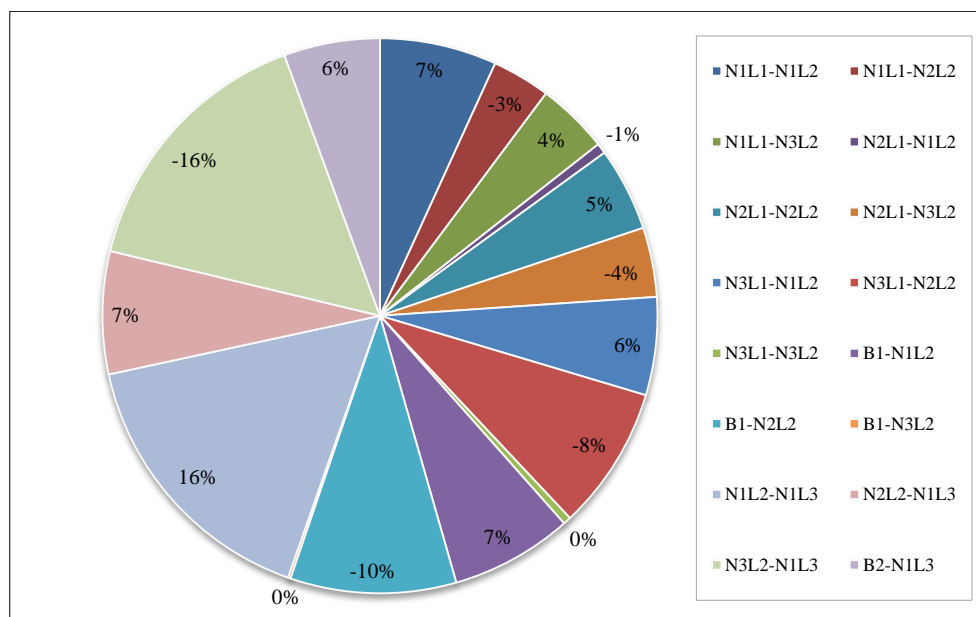**Figure 4. Artificial neural network structure of local scour**

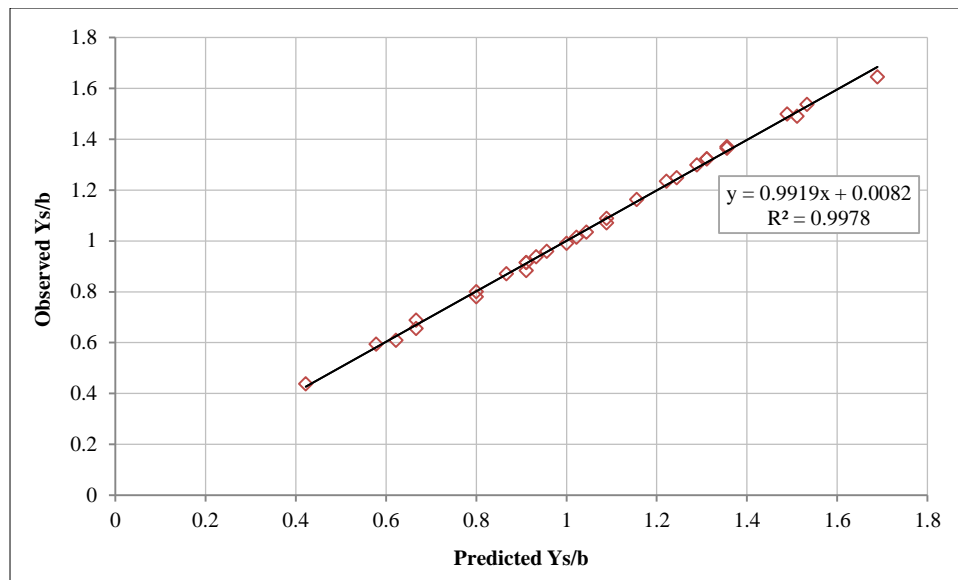**Figure 5. Pie chart distribution results of neural connection weights**

Figure 6. Predicted- Observed fitted line of ANN Results

5. Gene Expression Programming

Ferreira (2001) [29] is the one who came up with the idea of Gene Expression Programming, which is a genetic algorithm in which individuals are encoded as symbolic strings of a predetermined length (genotype), and they are then expressed as expression trees of various sizes and shapes. Ferreira (2001) [29] says that this method combines the good things about GA and GP while avoiding some of the bad things about each.

The results of previous experiments suggest that basic GEP can be used for economic prediction and still produce reasonable outcomes. On the other hand, just like with other fundamental evolutionary algorithms, the performance is highly dependent on the size of the population. The use of a smaller population size will result in a reduction in the diversity of the population as well as a reduction in the amount of pressure that individuals are under to compete with one another. This will lead to a reduction in the search space and an impairment of performance. Additionally, selecting a larger population size will require a longer execution time, which will have an impact on the algorithm's overall effectiveness. It's possible that the performance was affected by some other factors as well, such as the value of genetic operators [30].

Gene Expression Programming results can be seen in Figure 7 expressed as expression tree for local scour, and the gene expression structure tree expressed in Equation 7:

$$Y_s/b = K_{sh} \times (V/V_c) \times \min[K_{sh}, (V/V_c)] + \min\left[(Fr_p/K_{sh})/2), K_{sh} \times (V/V_c)\right] \tag{7}$$
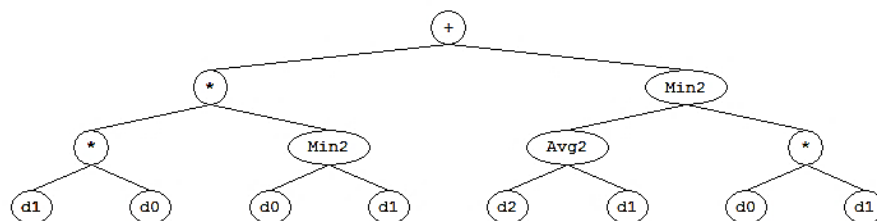

Figure 7. Gene expression structure of local scour

6. CFD Results

Al-Shukur & Obeid (2016) [17] studied the prediction of scour depth around bridge piers by using CFD code. They used ten different uniform pier shapes. The pier properties are as discussed in the literature. They simulated the free surface flow with the volume of fluid (VOF) technique [31, 32], which was concluded by Hirt & Nichols (1975) [33] and more completely in Hirt & Nichols (1981) [34]. In their paper, they set the boundaries as follows:

- Inlet as specified velocity of 0.3 m/s and depth of water of 12 cm.

- Outlet as an outflow.

- Top boundary as specified pressure and bottom and sides as solid walls boundaries. The wall boundary is considered as no-slip for processed by standard wall function.

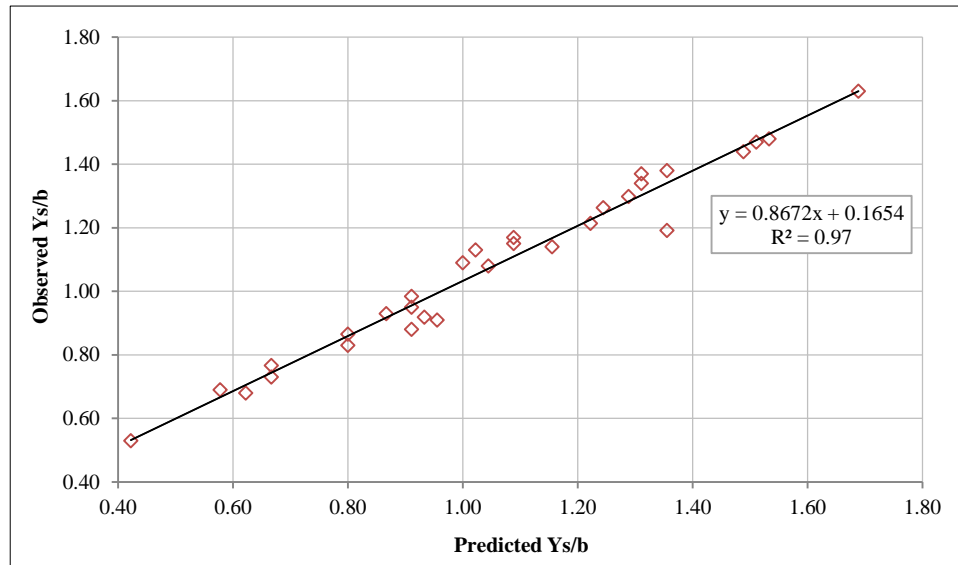Figure 8 illustrates the predicted- observed fitted line of CFD model with R² = 0.97.

Figure 8. Predicted- Observed fitted line of CFD Results

7. Statistical Analyses

In order to have confidence in the results of any model, the statistical analyses should take this into account to ensure the efficiency and adequateness of these results. To understand the behaviour of all independent variables and their relationships with the dependent variable, the scour depth results of each model were studied and analyzed statistically with the benefit of some performance measures and the goodness of fit test; these measures can be summarized in Equations 8 to 13:

- Mean Square Error:

$$MSE = \sum (X - Y)^2 / N \tag{8}$$

- Root Mean Square Error:

$$RMSE = \sqrt{MSE} = \sqrt{\sum (X - Y)^2 / N} \tag{9}$$

- Relative Square Error:

$$RSE = \sum (X - Y)^2 / \sum (\overline{Y} - Y)^2 \tag{10}$$

- Root Relative Square Error:

$$RRSE = \sqrt{RSE} = \sqrt{\sum (X - Y)^2 / \sum (\overline{Y} - Y)^2} \tag{11}$$

- Mean Absolute Error:

$$MSE = \sum |(X - Y)| / N \tag{12}$$

- Relative Absolute Error:

$$RSE = \sum |(X - Y)| / \sum |(\overline{Y} - Y)| \tag{13}$$

where, *X* represents the observed values, *Y* represents the estimated values, *N* represents the number of values and $\overline{Y}$ represents the mean of estimated values. Where the goodness of fit test results shown in Table 2.

Table 2. Goodness of fit test results

Parameter	GENE	ANN	MNLR	CFD
MSE	1.41E-03	2.16E-04	7.29E-03	3.70E-03
RMSE	3.75E-02	1.47E-02	8.54E-02	6.09E-02
RSE	1.36E-02	2.31E-03	1.10E-01	4.96E-02
RRSE	1.17E-01	4.81E-02	3.31E-01	2.23E-01
MAE	2.67E-02	1.16E-02	7.16E-02	5.33E-02
RAE	1.02E-01	4.54E-02	3.23E-01	2.30E-01
R²	9.80E-01	9.90E-01	9.60E-01	9.70E-01

Goodness of fit test considered one of the most commonly used tests, this test depending on the ratio of summations square error and it can be represented by the coefficient of determination R^2. The coefficient of determination can be defined as a mathematical model that deals with the ratio of errors resulting from observed data to errors resulting from predicted data, as shown in Equation 14.

$$R^2 = 1 - (X - Y)^2 / (X - \bar{X})^2 \tag{14}$$

where, X represents the observed values, Y represents the estimated values and $\bar{X}$ represents the mean of observed values

8. ANN, MNLR, and GEP Results Comparison

The observed experimental data on the scour depth around bridge piers compared with that predicted from the models generated by both the ANN, MNLR CFD, and GEP approaches. Figure 9 shows a comparison between Ys/b values that results from various approaches used in this study, namely, observed, CFD, MNLR, ANN, and Gene. The results showed good agreement between the approaches used. Where the results obtained from the use of different approaches agreed well with the observed data.
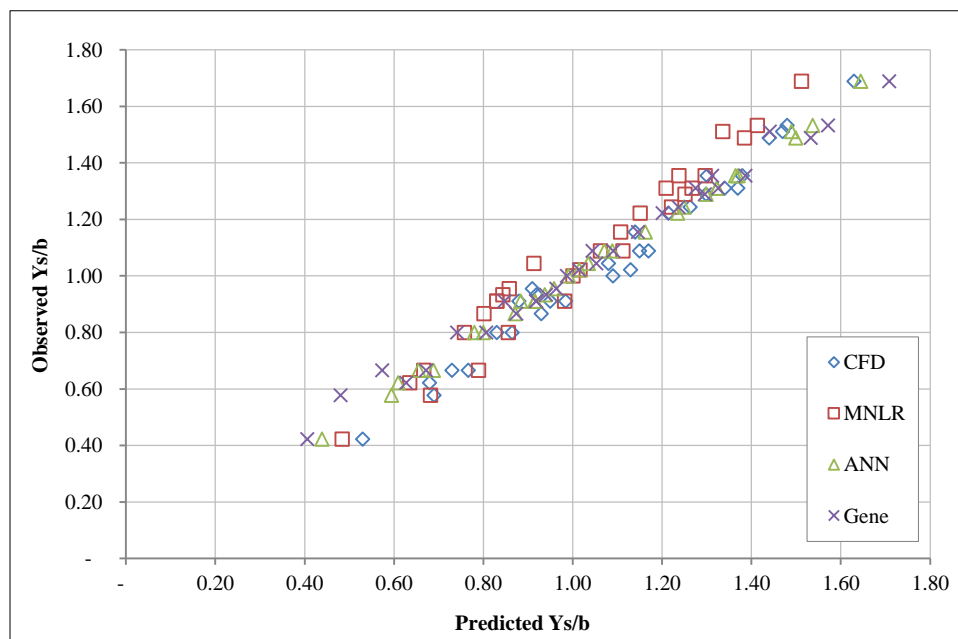

Figure 9. Observed data, CFD, MNLR, ANN and Gene Results Comparison of Ys/b

The comparison of values that measured and predicted by the four models CFD, MNLR, ANN, and Gene, it is seen that the ANN model has the ability to predict the Ys/b values higher than other models used in relation to the measured values. This makes the ANN model more superior for predicting the Ys/b value over the other used models, followed by the Gene model. In comparison the values of the R^2 and RMSE for the four models that used in this study, for Ys/b model by using the ANN have a value of R^2 and RMSE of 0.9978 and 0.0147, respectively while that of Ys/b by using Gene model were 0.9800 and 0.0375, respectively, other approaches results shown in Table 1. It gives an indication that the actual relationship between the selected variables in this study was sufficiently represented by using the ANN and Gene models that obtained compared to the other used models. It as well shows the ability of ANN model on predict 99.78% of the total variation in the CFD which was attributed to the studied variables in this study, and the Gene model predicted about 98.0% of the total variation in the Ys/b. This also, confirms that the ANN model is more accurate in data fitting compared to the other used models. Depending on the R^2 and RMSE values and other tested parameters, the ANN model has very good accuracy, more than that of the CFD, MNLR, ANN, and Gene models, which are followed by the Gene, CFD, and MNLR models, respectively.

Figure 10 illustrates the relationship between Ys and Frp for different pier shapes. It is clear from this relation that the accuracy of the results for all the discharges is similar, but the closest for the observed data are ANN and Gene.
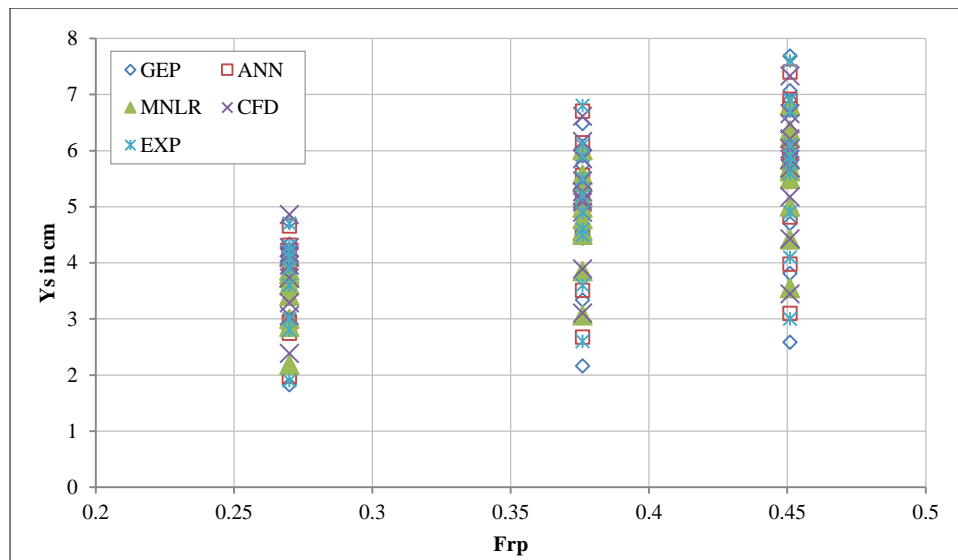
Figure 10. Results of Gene, ANN, MNLR, CFD approaches for different flow rates

9. Conclusion

Excessive localized erosion around bridge piers can cause a variety of issues for the structure of the bridge as a whole, including issues with its stability, and may even result in the bridge's complete destruction. Because of this, the scour effect needs to be studied carefully in order to find a solution to this issue, particularly given the fact that the collapse of the bridge could result in the deaths of a large number of people. The purpose of this paper is to verify the scour depth around different shapes of uniform bridge piers for different flow conditions that were done by Al-Shuker & Obeid (2016) by using a variety of different prediction models. The reliability of the experimental investigation described in Al-Shuker & Obeid (2016) is checked using multiple nonlinear regression analysis (MNLR), gene expression programming (GEP), and artificial neural network (ANN) models. The result of Ys/b that was obtained from the prediction models that were used was validated and compared with the data that was observed regarding Ys/b. More so than the Gene, CFD, and MNLR models, the ANN model did an outstanding job of representing the data and came extremely close to the actual data that was observed. This article shows how techniques like CFD, MNLR, ANN, and Gene can be used in everyday life to make accurate predictions about the global water system.

10. Declarations

10.1. Author Contributions

Conceptualization, S.A. and H.I.A.; methodology, S.A.; software, H.I.A.; validation, S.A., H.I.A., and A.A.A.; formal analysis, T.M.H.; investigation, H.I.A.; resources, S.A.; data curation, H.I.A.; writing—original draft preparation, A.A.A. and T.M.H.; writing—review and editing, T.M.H.; visualization, T.M.H.; supervision, H.I.A.; project administration, H.I.A.; funding acquisition, H.I.A. All authors have read and agreed to the published version of the manuscript.

10.2. Data Availability Statement

The data presented in this study are available on request from the corresponding author.

10.3. Funding

The authors received no financial support for the research, authorship, and/or publication of this article.

10.4. Conflicts of Interest

The authors declare no conflict of interest.

11. References

[1] Richardson, E. V., & Davis, S. R. (2001). Evaluating scour at bridges. No. FHWA-NHI-01-001. Office of Bridge Technology, Federal Highway Administration, Washington, United States.

[2] Melville, B. W., & Coleman, S. E. (2000). Bridge scour. Water Resources Publication, Colorado, United States.

[3] Arneson, L. A., Zevenbergen, L. W., Lagasse, P. F., & Clopper, P. E. (2012). Evaluating scour at bridges. No. FHWA-HIF-12-003, National Highway Institute, Washington, United States.

[4] Hamil, L. (1999). Bridge Hydraulics. Taylor & Francis, Milton Park, United States.

[5] Chiew, Y. M. (1984). Local Scour at Bridge Piers. Ph.D. Thesis, Department of Civil Engineering, The University of Auckland, Auckland, New Zealand.

[6] Barbhuiya, A. K., & Dey, S. (2003). Vortex flow field in a scour hole around abutments. International Journal of Sediment Research, 18(4), 310-325.

[7] Laursen, E. M., & Toch, A. (1956). Scour around bridge piers and abutments (Vol. 4). Ames, Iowa Highway Research Board, Iowa, United States.

[8] Neil, D. T., Orpin, A. R., Ridd, P. V., & Yu, B. (2002). Sediment yield and impacts from river catchments to the Great Barrier Reef lagoon: a review. Marine and Freshwater Research, 53(4), 733-752. doi:10.1071/MF00151.

[9] Dietz, J. W. (1972). Construction of long piers at oblique currents illustrated by the BAB-Main Bridge Eddersheim, and Systematic model tests on scour formation at piers. Mitteilungsblatt der Bundersanstalt for Wasserbau, 31.

[10] Melville, B. W. (1975). Local scour at bridge sites. Report. No. 117, School of Engineering, University of Auckland, Auckland, New Zealand.

[11] Komura, S., Neill, C. R., & Breusers, H. N. C. (1963). Discussion of "Sediment Transportation Mechanics: Erosion of Sediment: Progress Report by the Task Committee on Preparation of Sedimentation Manual of the Committee on Sedimentation of the Hydraulics Division". Journal of the Hydraulics Division, 89(1), 269-281.

[12] Omara, H., Ookawara, S., Nassar, K. A., Masria, A., & Tawfik, A. (2022). Assessing local scour at rectangular bridge piers. Ocean Engineering, 266, 112912. doi:10.1016/j.oceaneng.2022.112912.

[13] Luo, K., Si, Y., Lu, S., Liang, B., & Qi, H. (2022). Characteristics of reducing local scour around cylindrical pier using a horn-shaped collar. Journal of Engineering and Applied Science, 69(1), 1-21. doi:10.1186/s44147-022-00160-x.

[14] Reddy, S. K., Kalathil, S. T., Chand, M. G., & Chandra, V. (2022). Influence of Pier Shape and Interference Effect on Local Scour. River Hydraulics, 297-307. doi:10.1007/978-3-030-81768-8_25.

[15] Farooq, R., & Ghumman, A. R. (2019). Impact assessment of pier shape and modifications on scouring around bridge pier. Water, 11(9), 1761. doi:10.3390/w11091761.

[16] Jan, R., & Lone, M. A. (2022). Effect of mutual interference of piers on their local scour phenomenon. Innovative Infrastructure Solutions, 7(2), 1-15. doi:10.1007/s41062-022-00790-3.

[17] Al-Shukur, A. H. K., & Obeid, Z. H. (2016). Experimental study of bridge pier shape to minimize local scour. International Journal of Civil Engineering and Technology, 7(1), 162-171.

[18] Moussa, A. M. A. (2018). Evaluation of local scour around bridge piers for various geometrical shapes using mathematical models. Ain Shams Engineering Journal, 9(4), 2571–2580. doi:10.1016/j.asej.2017.08.003.

[19] Vijayasree, B. A., Eldho, T. I., Mazumder, B. S., & Ahmad, N. (2019). Influence of bridge pier shape on flow field and scour geometry. International Journal of River Basin Management, 17(1), 109–129. doi:10.1080/15715124.2017.1394315.

[20] Canadian Standards Association (CSA). (2019). Canadian Highway Bridge Design Code; CSA S6-19 833. Canadian Standards Association (CSA), Toronto, Canada.

[21] Jalal, H. K., & Hassan, W. H. (2020). Effect of Bridge Pier Shape on Depth of Scour. IOP Conference Series: Materials Science and Engineering, 671(1), 12001. doi:10.1088/1757-899X/671/1/012001.

[22] Aly, A.M., & Dougherty, E. (2021). Bridge pier geometry effects on local scour potential: A comparative study. Ocean Engineering, 234, 109326. doi:10.1016/j.oceaneng.2021.109326.

[23] Ghodsi, H., Najafzadeh, M., Khanjani, M. J., & Beheshti, A. (2021). Effects of Different Geometric Parameters of Complex Bridge Piers on Maximum Scour Depth: Experimental Study. Journal of Waterway, Port, Coastal, and Ocean Engineering, 147(5), 4021021. doi:10.1061/(asce)ww.1943-5460.0000645.

[24] Melville, B.W., & Sutherland, A.J. (1988). Design Method for Local Scour at Bridge Piers. Journal of Hydraulic Engineering, 114(10), 1210–1226. doi:10.1061/(asce)0733-9429(1988)114:10(1210).

[25] Raudkivi, A.J., & Ettema, R. (1983). Clear-water scour at cylindrical piers. Journal of hydraulic engineering, 109(3), 338-350. doi:10.1061/(ASCE)0733-9429(1983)109:3(338).

[26] Riahi-Madvar, H., Dehghani, M., Seifi, A., Salwana, E., Shamshirband, S., Mosavi, A., & Chau, K.W. (2019). Comparative analysis of soft computing techniques RBF, MLP, and ANFIS with MLR and MNLR for predicting grade-control scour hole geometry. Engineering Applications of Computational Fluid Mechanics, 13(1), 529-550.

[27] IBM SPSS Statistics. (2018). IBM SPSS Statistical v22 Commend Syntax Reference. Available online: https://www.ibm.com/support/pages/ibm-spss-statistics-22-documentation (accessed on May 2022).

[28] Shakya, R., Singh, M., Sarda, V. K., & Kumar, N. (2022). Scour depth forecast modeling caused by submerged vertical impinging circular jet: a comparative study between ANN and MNLR. Sustainable Water Resources Management, 8(2), 1-10. doi:10.1007/s40899-022-00634-z.

[29] Ferreira, C. (2001). Gene expression programming: a new adaptive algorithm for solving problems. arXiv preprint. doi:10.48550/arXiv.cs/0102027.

[30] Li, Q., Cai, Z., Zhu, L., & Zhao, Y. (2004). Application of gene expression programming in predicting the amount of gas emitted from coal face. Yingyong Jichu Yu Gongcheng Kexue Xuebao/Journal of Basic Science and Engineering, 12(1), 49–54.

[31] Al Shaikhli, H. I., & S. I. Khassaf (2022). Using of flow 3d as CFD materials approach in waves generation. Materials Today: Proceedings, 49, 2907–2911. doi:10.1016/j.matpr.2021.10.282

[32] Al Shaikhli, H. I., & Khassaf, S. I. (2022). Stepped Mound Breakwater Simulation by Using Flow 3D. Eurasian Journal of Engineering and Technology, 6, 60-68.

[33] Hirt, C. W., Nichols, B. D., & Romero, N. C. (1975). SOLA: A numerical solution algorithm for transient fluid flows (No. LA-5852). Los Alamos Scientific Lab., New Mexico, United States.

[34] Hirt, C. W., & Nichols, B. D. (1981). Volume of fluid (VOF) method for the dynamics of free boundaries. Journal of Computational Physics, 39(1), 201–225. doi:10.1016/0021-9991(81)90145-5.